Research

Author for correspondence:
Miriam Beck
e-mail: miriam.beck@imev-mer.fr

THE ROYAL SOCIETY PUBLISHING

Morphological diversity increases with decreasing resources along a zooplankton time series

Miriam Beck[1], Caroline Cailleton[1], Lionel Guidi[1], Corinne Desnos[2], Laetitia Jalabert[2], Amanda Elineau[2], Lars Stemmann[1], Sakina-Dorothée Ayata[3,4,†] and Jean-Olivier Irisson[1,†]

[1]Sorbonne Université, CNRS, Laboratoire d'Océanographie de Villefranche, LOV, 06230 Villefranche-sur-Mer, France
[2]Sorbonne Université, CNRS, Institut de la mer de Villefranche, IMEV, 06230 Villefranche-sur-Mer, France
[3]Sorbonne Université, CNRS, IRD, MNHN, Laboratoire d'Océanographie et du Climat: Expérimentation et Analyses Numériques, LOCEAN-IPSL, 75005 Paris, France
[4]Institut Universitaire de France (IUF), 75005 Paris, France

MB, 0000-0001-8179-3820

Biodiversity is studied notably because of its reciprocal relationship with ecosystem functions such as production. Diversity is traditionally described from a taxonomic, genetic or functional point of view but the diversity in organism morphology is seldom explicitly considered, except for body size. We describe morphological diversity of marine zooplankton seasonally and over 12 years using quantitative imaging of weekly plankton samples, in the northwestern Mediterranean Sea. We extract 45 morphological features on greater than 800 000 individuals, which we summarize into four main morphological traits (size, transparency, circularity and shape complexity). In this morphological space, we define objective morphological groups and, from those, compute morphological diversity indices (richness, evenness and divergence) using metrics originally defined for functional diversity. On both time scales, morphological diversity increased when nutritive resources and plankton concentrations were low, thus matching the theoretical reciprocal relationship. Over the long term at least, this diversity increase was not fully attributable to taxonomic diversity changes. The decline in the most common plankton forms and the increase in morphological variance and in extreme morphologies suggest a mechanism akin to specialization under low production, with likely consequences for trophic structure and carbon flux.

1. Introduction

Numerous studies indicate that in aquatic and terrestrial ecosystems biodiversity is positively linked to productivity, for example, reporting increasing primary production due to increased resource use efficiency [1,2]. Biodiversity is in turn influenced by the overall production of a system, as shown by the linear decline in taxonomic richness of phyto- and zoo-plankton when nutrient concentrations increase [3]. Still, in arctic soft bottom communities, the relationship seem to be more complex: while invertebrate diversity decreased at high production levels, it was also low at very low production levels, resulting in a unimodal shape on a local scale [4]. Also, a plankton community study [5] and a meta-analysis [6] revealed varying slopes in this relationship, depending on the spatial scale and organism type, underlining the context-dependence and complex mechanisms acting on it.

Depending on the question addressed, biodiversity is quantified by various indices describing, for example, taxonomic, phylogenetic or functional diversity. The latter, relying on functional traits instead of taxonomic identity, captures the range of ecological strategies present at a site and is thus directly

linked to ecosystem functioning [7,8]. This allows insights often not captured when relying solely on taxonomic indices. For instance, in winter, a phytoplankton community can remain functionally diverse despite declining taxonomic richness [9] and plant assemblages can experience a substantial loss in functional diversity over the long term, although species richness increases [10]. The taxonomic and functional approaches thus complement each other and provide a better understanding of community structuration by identifying ecological processes such as competitive exclusion [11] or functional homogenization [12].

Among the commonly used functional traits, morphological traits, describing part of the phenotype of an organism, are scarcely considered, except for body size. Indeed, the latter is considered a 'master trait', since most physiological rates, e.g. metabolism [13,14], growth or feeding [15] scale with size. Size itself is affected by environmental conditions and, for example, warming and nutrient enrichment locally increased the proportion of small phyto- and zoo-plankton, macroinvertebrates and fish, at both species and community levels [16–18]. Such shifts in the size structure of a community, with consequences on its functioning, can occur with no change in taxonomic diversity. This was documented for benthic macroinvertebrates for which a lower proportion of large organisms decreased decomposition rates without affecting Shannon diversity and evenness [19]. The positive relationship between predator size and the intensity of trophic cascades is another example of how body size influences food web structure and energy flux [20]. Using morphological features beyond size, Marinello & Bernhard [21] showed that wing shape of bats can be a proxy for their flight pattern and feeding strategy, with carnivores having rather short, round wings of a large surface allowing them to lift and carry prey. Sonnet et al. [22] found a negative correlation of phytoplankton shape complexity and size with nutrient concentration, which suggests that considering phytoplankton shape can improve our understanding of the seasonal succession.

Compared with other phenotypic characteristics, morphological information can easily be captured by images. Its measurement can then be automated through machine learning [23], which provides large quantities of objective data. The increasing use of imaging techniques for plankton [24] makes this group attractive to integrate morphological features into ecological analyses. Such techniques enabled Vilgrain et al. [25] to quantify reproduction, feeding behaviour, gut fullness and pigmentation of copepods at individual level, revealing clear patterns over scales of dozens of kilometres and providing insight into the functioning of planktonic ecosystems during the ice break-up in the Arctic. In mosquitofish, measurements of morphological traits including eye position, head size and elongation confirmed expected differences between individuals in high- and low-predator environments, which enhance swimming performance under predator pressure [26].

Ecosystem functioning worldwide is, and will continue to be, affected by climate change (IPBES and IPCC; [27]). Beyond temperature rise, indirect consequences of warming on marine environments include reduced nutrient and oxygen availabilities in surface layers [28] and a global decline in primary production and animal biomass [29,30]. Many marine ecosystems will experience drastic species turnover [31] with smaller organisms and/or taxa probably favoured in most cases [32–34]. Increasing nutrient concentrations often cause functional and/or taxonomic homogenization through the dominance of generalist taxa [35–37], suggesting community shifts towards specialists and increasing diversity with oligotrophication, as already observed for a stream phytoplankton community over 34 years [38].

In the Mediterranean Sea, a hotspot of climate change, many regions endure multiple stressors, such as increasing temperature and salinity, extreme events and continuing oligotrophication [39,40]. Investigating ecosystem responses to climate change in this area hence both important and informative. In the northwestern basin, temperature increased while nutrients declined over the last two decades [41]. We thus expect zooplankton in this region to respond with increased morphological diversity due to species turnover and/or intraspecific variations as the community shifts towards individuals with more specialized morphologies under increasingly oligotrophic conditions. To test this hypothesis, we quantified zooplankton morphological diversity on seasonal and inter-annual time scales, along a 12-year times series collected at a site in the northwestern Mediterranean. We synthesized the morphological features from greater than 800 000 images of individual zooplanktonic organisms and defined groups of morphologically similar individuals. Based on these 'morphs' we characterized morphological diversity and investigated the impact of environmental drivers.

2. Material and methods

(a) Sampling

Zooplankton and environmental variables were sampled at 'point B', near the entrance of the bay of Villefranche-sur-mer (France, northwestern Mediterranean Sea, 43°41′06.0″ N, 7°18′56.4″ E). The bay is largely open to waters and plankton from the open sea since it is the tip of a 2000 m deep submarine canyon. Zooplankton was sampled in mornings and afternoons of each working day, from 1 July 2009 to 12 December 2020. Samples were taken with a WP2 net (200 μm mesh size), hauled vertically from 75 m depth to the surface (approx. 18.75 m³ of seawater filtered per haul). Samples were fixed with formalin buffered with borax before further treatment. At the same site, the following environmental variables: water temperature (°C), salinity (practical salinity units (PSU)), dissolved oxygen (ml l^{-1}), nitrate (NO_3^-; μmol l^{-1}), nitrite (NO_2^-; μmol l^{-1}), phosphate (PO_4^{3-}; μmol l^{-1}), chlorophyll a (μg l^{-1}), pH, particulate organic carbon and particulate organic nitrogen (POC, PON; μg l^{-1}), were measured once per week, in the morning, at six depths, as part of the SOMLIT network following standardized protocols (http://somlit.fr). To match biological and environmental samples in frequency and sampling depth, zooplankton samples were pooled per week while environmental variables were integrated between 75 m and the surface.

The workflow summarizing the steps from the imaged individuals to the quantification of diversity are displayed in figure 1.

(b) Quantitative imaging

Zooplankton samples were fractionated on a 1 mm filter to separate large and small objects. Each fraction was subsampled (at 1/2, 1/4, 1/8 etc.) using a Motoda splitting box [42] until approximately 1000 objects could be digitized using the ZooScan, a scanner designed for zooplankton. Scanned images (1 pixel = 10.6 μm) were automatically processed to extract and
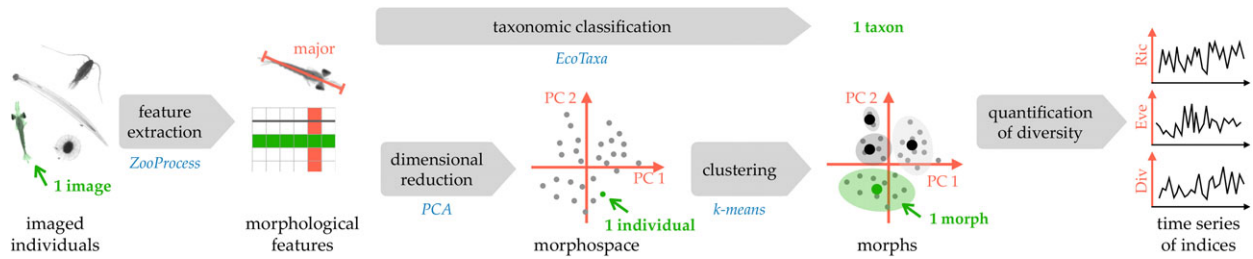
Figure 1. Workflow from individual images to the quantification of diversity. Green font indicates the object handled in the next step; red a variable; blue the method or software.

measure all objects with the ZooProcess software [43]. In total, 45 morphological features were extracted (electronic supplementary material, S1; figure 1). They were related to size (e.g. perimeter, area, size of smallest rectangle or ellipse surrounding the object), shape (e.g. circularity, elongation, perimeter complexity), and the distribution of grey levels (e.g. contrast, minimum grey, modal grey). Images showcasing processing artefacts such as undersegmentation (two touching objects considered as one) were removed. Individual objects and their associated measurements were uploaded to the EcoTaxa platform for taxonomic identification [44]. Identifications were reviewed by several experts for the entire time series, to ensure consistency. In total, 44 taxa were identified with taxonomic levels ranging from species (only few) to broader taxonomic groups (e.g. Amphipoda, Ostracoda; full list in electronic supplementary material, S2). Juvenile and larval stages were treated separately when appearing in high numbers and otherwise were grouped with adults of their taxa. Zooids of colonial taxa were treated as the identified taxon. Largely incomplete objects (i.e. body parts) and rare taxa (appearing with $n < 100$ out of a total of $n = 845\,812$ individuals over the whole time series) were excluded from the analysis. Samples with high numbers of scanned objects ($n > 2000$ for the sum of the two scans) were randomly sub-sampled ($n = 2000$) to avoid differences in imaging effort possibly influencing the assessment of diversity. The concentration of each taxon in each sample (individuals m^{-3}) was calculated based on the image count, the Motoda fraction and the filtered water volume.

(c) Morphological space and definition of 'morphs'

The 45 morphological features were summarized through an observation-weighted principal component analysis (PCA; figure 1) computed on the 845 812 imaged individuals. Each image was weighted by its 'individual' concentration to be representative of its importance in the water rather than on the scan, hence erasing differences in Motoda fractionating rate or volume sampled at sea among weeks. The PCA synthesized their correlation and allowed placing each individual in a reduced 'morphological space'. To ensure the applicability of PCA, histograms of each morphological feature were checked prior to the analysis. When necessary, outliers were removed by censoring the lower and/or upper 0.1% of the feature values. For not-normal distributions, a log transformation was applied to increase symmetry. Electronic supplementary material, table S1 details what was applied to each feature. After censoring, individuals with more than five removed values ($n = 1448$) were considered too extreme and excluded from the analysis. Other missing values (affecting $n = 20\,986$ individuals) were replaced by the mean of the corresponding feature, which is neutral in PCA. The number of PCA axes worthy of further examination was determined by judging the scree plot. Each of the selected PCA axes was then interpreted as a morphological trait, with a meaning defined according to the morphological features most associated with it. To follow the

variation in morphology within the community over time, for each date, we calculated the mean, standard deviation, 0.25 and 0.75 quantile of individuals' coordinates along each axis.

Finally, groups of morphologically similar individuals (i.e. 'morphs') were defined, to be then used to quantify morphological diversity: observation-weighted k-means clustering [45] was applied on the individuals' coordinates along the selected PCA axes (figure 1); weights were again the 'individual' concentrations. The number of clusters was set to 200, which was identified as a good compromise between the resolution in the definition of morphs and their generality; defining 400 morphs only marginally changed the results. Morphs differed from taxa, since one morph comprised on average 15 taxa (ranging from 5 to 30) and each taxon appeared on average in 70 morphs (ranging from 5 for Pyrosomatida to 197 for Copepoda). For each date, the concentration of each morph was calculated as the sum of the concentrations of all individuals belonging to that morph.

(d) Quantifying morphological and taxonomic diversity

Villéger et al. [46] developed three indices describing different and complementary aspects of functional diversity: richness, regularity and divergence. Using 'morphs' and their average morphological traits, instead of species and their average functional traits, we used those indices to quantify morphological diversity. Each index was calculated for each date, based on the position of the barycentre of each morph in the reduced morphological space (= the centroids of the k-means clusters) and its concentration (= sum of the 'individual' concentrations of cluster members) at that date. Morphological richness (MRic) represents the proportion of the total morphological diversity present at a given date. It is calculated as the volume of the convex hull enclosing all the morph's centroids present at that certain date. Thus, it does not take the morphs' concentrations into account and rather depends on the most extreme morphs. Morphological evenness (MEve), or regularity, is a measure of the homogeneity of the differences in appearances between morphs present at a given date. It is high if the appearance changes gradually between morphs; it is low if some morphs are very different from other morphs that are similar to each other. Numerically, the minimum spanning tree between the present morphs calculated and the equidistance along the branches of this tree defines the morphological regularity. Finally, morphological divergence (MDiv) quantifies morphological dissimilarity within the fraction of diversity present at a given date. MDiv is high when several morphs of very different appearance are abundant; it is low when the abundant morphs are morphologically similar. First, the gravity centre of morphs present at the target date was computed. Then, the distances from each morph to this gravity centre as well as their average were computed. The index is based on the sum of the anomalies of theses distances compared with their mean. Since everything is computed based only on the morphs present at a given date, the index quantifies morphological divergence within a certain level of diversity (i.e. richness).

Taxonomic diversity was quantified by calculating taxonomic richness (i.e. number of taxa present, TRic), Pielou Evenness (TEve ; [47]) and Shannon Diversity (TDiv; [48]).

(e) Times-series analysis

All time series were processed equally: morphological and taxonomic diversity indices, environmental variables, total zooplankton concentration and morphological change in the community (mean, standard deviation, 0.25 and 0.75 quantiles). Values missing over short periods (1–2 weeks; $n = 2$–3 per year) were filled by linear interpolation of the original variable. For gaps spanning a period greater than or equal to 3 weeks ($n = 1$ in beginning of 2017) missing values were interpolated by the analysis technique described hereafter. The seasonal component was extracted by seasonal-trend decomposition by Loess (STL; [49]). Since different de-seasonalizing methods within STL provided very similar results, we kept the simplest one and assumed seasonal component to be identical over all years ('periodic' signal).

After removing this seasonal signal, the significance of the long-term trend was tested using a generalized least squares (GLS) linear regression with a first-order autoregressive correlation structure in the residuals [50]. This level of auto-correlation was determined by examining the partial auto-correlogram of the residuals of a simple linear model. The assumptions of the linear model (normality, homoscedasticity) were then tested on the de-correlated residuals. When the assumptions were not met, the process was repeated on transformed data (e.g. $\log(n + 1)$ for zooplankton concentrations). While changes are not likely to be completely progressive and linear over the whole period (they may rather occur more intensely at some periods), this approach was used as a parsimonious way of statistically testing for overall changes.

The definition of a morphological space and morphs, quantification of diversity and time-series analyses were repeated considering only the copepods within the community ($n = 649\,825$ images), to investigate whether the results persisted in a more taxonomically homogeneous community.

(f) Software

All analyses were performed using R 3.4.4 [51] and the following packages: ade4 1.7–10 [52] for weighted PCA, vegan 2.4–6 [53] for calculating the Pielou and Shannon indices, pastecs 1.3–18 [54] for interpolation and calculation of moving averages on time series, stlplus 0.5.1 [55] for STL decomposition, nlme 3.1–131.1 [56] for GLS regression, dplyr 0.7.4 [57] for data manipulation, and ggplot2 2.2.1 [58] and factoextra 1.0.7 [59] for graphics. The representation of the morphological space (figure 2) was coded in https://github.com/jiho/morphr/ and the computation of observation-weighted k-means was coded in https://github.com/jiho/wkmeans. The morphological diversity indices were calculated after optimizing the functions of Sébastien Villéger (http://villeger.sebastien.free.fr/Rscripts.html). The entire code used for the analyses is available for reproducibility, at https://github.com/jiho/ptb_morphodiv.

3. Results

(a) Description of the morphological space

The morphological space was built by the first four axes of the PCA on morphological features, which explain together 75.39% of the total variance of zooplankton morphology (37.86%, 21.29%, 9.4% and 6.84%, respectively) and represent the main morphological traits of the community. The first axis (PC1) mainly captured changes in body size (figure 2).

The second axis (PC2) can be interpreted as transparency separating light, i.e. transparent, individuals with homogeneous grey levels from darker and more contrasted individuals. The third axis (PC3) separated individuals by their circularity and symmetry, opposing elongated individuals with a marked bilateral symmetry and more circular ones. Finally, the fourth axis (PC4) quantified shape complexity and separated individuals with a simple perimeter from those with more complex contours.

Taxonomically, Limacinidae (Gastropoda) and Bivalvia dominated the lower end of the size continuum and Salpida and Chaetognatha dominated the upper end (electronic supplementary material, S2). The transparency axis separated gelatinous taxa, such as Appendicularia (Fritillariidae, Oikopleuridae) and Chaetognatha from opaque, carapace-bearing (Eumalacostraca, Copepoda, Amphipoda) or shell-bearing (Gastropoda like *Cavolinia inflexa*) zooplankton. Chaetognatha and *Creseis acicula* (Gastropoda) expressed the highest elongation, while Salpida, Phaeodarea and pieces of *Abylopsis tetragona* (Siphonophorae) belonged to the most circular individuals. Taxa with simpler outlines were Salpida, Chaetognatha and Diphyidae (Siphonophorae), while the most complex shapes were observed for Echinodermata larvae, Phaeodarea and Copepoda with antennae in open position.

(b) Seasonality in zooplankton and environmental conditions

The seasonal component showed the typical succession of a plankton bloom: Chlorophyll *a* concentration peaked in March, followed by zooplankton concentration peaking in the beginning of April (figure 3). Temperature increased towards summer, while nutrient and particle concentrations declined, starting just before the chlorophyll peak for some (e.g. PO_4^{3-}, NO_3^-) or at the zooplankton peak for others (PON; figure 3; electronic supplementary material S3).

The pattern for taxonomic and morphological diversity was similar for all indices (richness, evenness, divergence): diversity was low during spring (March, April) before sharply increasing until July and remaining stable at a high level over summer. In autumn, taxonomic diversity indices started to decrease while their morphological counterparts remained at a high level until the next spring (figure 3). Diversity, which was minimal in spring, was negatively correlated to zooplankton concentration, which was maximal at that time (electronic supplementary material, S4).

(c) Long-term trends in zooplankton and environmental conditions

Seven of the eleven environmental variables showed significant trends over the 12-year period. Average temperature between 0 and 75 m increased significantly (+0.59°C in 12 years, assuming a linear increase, with $p < 0.05$), so did salinity (+0.11 PSU) and oxygen (+0.43 ml l^{-1}; table 1). Concentrations of phosphate (−0.02 mg l^{-1}), particulate organic carbon (−43.2 mg l^{-1}) and nitrogen (−2.28 mg l^{-1}) significantly declined (table 1). The concentrations of nitrite, nitrate and silicate, as well as density, did not show a significant monotonous trend over the 12 years. The concentration of chlorophyll *a* significantly increased (+0.16 mg l^{-1}) while the total zooplankton concentration significantly declined during this period.
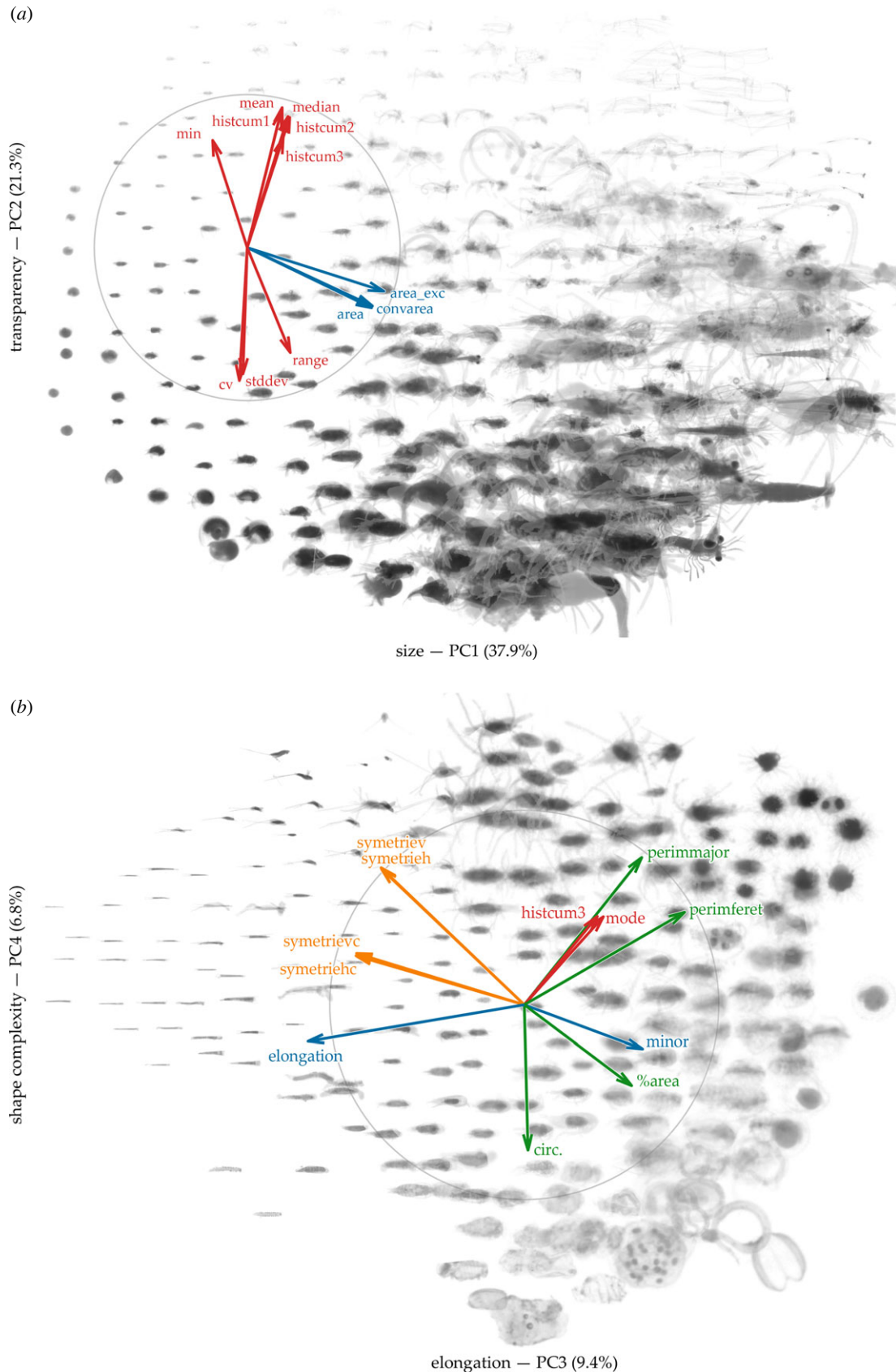
(a)

(b)

Figure 2. Zooplankton morphological space defined by the first four PCA axes, computed from 45 variables measured on 845 812 individual images. For each plane, only the 12 most contributing features are drawn. Features are coloured according to the morphological facet they capture: red for shades of grey, blue for size, orange for symmetry and green for other aspects of the shape. The variance captured by each axis and its interpretation in terms of synthetic morphological trait are indicated in the axis label. Images representative of a region of the morphological space were synthesized by combining three images randomly selected in the neighbourhood and the result was drawn on the plot.

In this context, taxonomic richness (TRic) significantly increased and the community became more morphologically diverse, both in terms of absolute (MRic) and relative (MDiv) diversity, i.e. the morphs present were more variable (figure 4 and table 1). There was no significant trend in morphological evenness (MEve)
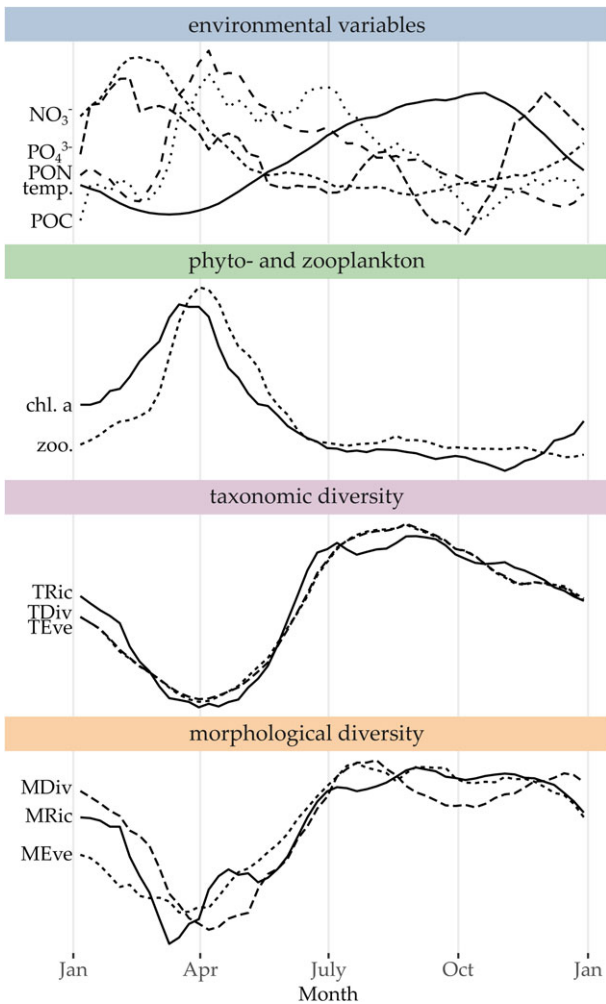
Figure 3. Seasonal component of environmental variables temperature, NO_3^-, PO_4^{3-}, POC, PON), zooplankton and chlorophyll *a* concentration (a proxy for the biomass of autotrophic phytoplankton), taxonomic and morphological diversity indices (richness, evenness, diversity/divergence). This component was derived by seasonal-trend decomposition by Loess over 2009–2020. Curves were smoothed with a moving average (window size = 5) and all variables were scaled and centred (mean = 0, variance = 1) for display.

($p > 0.05$, figure 4) and in taxonomic evenness (TEve) or diversity (TDiv).

The morphological traits of the community (i.e. the positions on the axes of the morphological space defined by the PCA) changed notably (table 1): the variance in size increased and the smaller individuals became smaller; the average and highly transparent organisms became more transparent and the overall variance in transparency increased; organisms became more elongated, both in average and at the extremes. Only shape complexity did not change significantly (table 1).

(d) Intra-taxon analysis of Copepoda

Analysing only Copepoda, the traits defining the morphological space were similar to those found for the entire zooplankton community: PC1 (36.46% of explained variance) and PC2 (19.77%) were size and transparency, respectively. The morphological interpretation of PC3 (8.94%) was less clear, but individuals with low scores on PC3 were more symmetric. PC4 (7.34%) was elongation (electronic supplementary material, S5).

As for the whole plankton community, copepod concentration peaked in April and then strongly declined (electronic supplementary material, S6). The three morphological diversity indices followed the opposite pattern: their values were lowest in April and increased over the year until July/August, fluctuating—more strongly than in case of the whole community—around intermediate values in late summer and autumn.

Over the 12 years, morphological richness and divergence of Copepoda increased significantly while their concentration declined (electronic supplementary material, S7), as observed for the entire zooplankton community. There was no significant trend in morphological evenness ($p > 0.05$). Significant trends in morphological traits were more variable sizes with notably more abundant smaller individuals, an increase in variance of transparency, and increases in average and extreme elongation values. The slope of these trends was similar or lower than those found for the entire community.

4. Discussion

Using morphological features derived from images, we successfully defined an interpretable morphological space comprising four synthetic traits: size, transparency, circularity and shape complexity. After defining objective groups of morphologically similar zooplankton, we detected both seasonal and long-term changes in morphological diversity indices computed from these groups. Over the spring–summer transition and over the 12-year study period, the total zooplankton concentration declined while the community became morphologically more diverse.

ZooScan imaging of preserved net samples allows the temporal decoupling of sampling and imaging, but comes with some limitations. First, the usual limitations of net-sampling still apply and the destruction of particularly fragile organisms can lead to an incomplete community description. In the target size range (200 µm to few centimetres), some Rhizaria and small jellies were probably missed. Second, the conservation of organisms with formalin can cause a temporary shrinkage of tissues in the days following fixation. Here, we scanned samples within weeks after collection (except for 2009 samples, which were processed in 2010) to minimize this bias and avoid further biases due to different storage periods. Finally, identifying organisms on images allows to process more of them than through manual microscopy but at the cost of a lower taxonomic resolution. In our study, taxa had to be aggregated to broader levels than what is possible to achieve from images to ensure consistency over the series. This limited the detection of taxonomic shifts that may have been visible at a finer taxonomic level. Nevertheless, it was sufficient to detect the seasonal shift in taxonomic diversity and an increase in taxa richness over the long term. A finer taxonomic resolution was available over the four most recent years. This was too short to perform a trend analysis, but the seasonal signal was very similar to that detected at the lower taxonomic resolution; only its amplitude was slightly affected (electronic supplementary material, S8).

(a) Seasonal variations of morphological diversity

On a seasonal scale, diversity and production were negatively correlated: all morphological and taxonomic diversity indices increased towards summer, while zooplankton concentration and nutrients declined. Besides a more diverse morphology,

Table 1. Trends in the zooplankton community (concentration, morphological and taxonomic diversity indices, values of morphological traits) and environmental variables over the 12-year period (2009–2020) obtained from generalized least squares (GLS) regression. For each index and variable, the slope describes the direction and intensity of the trend per year, the R^2 shows how much variance this linear model captures, and asterisks indicate significance with $p < 0.001$ (***), $p < 0.01$ (**) and $p < 0.05$ (*).

zooplankton				environment			
variable	slope	R^2	sig.	variable	slope	R^2	sig.
concentration	-74.6	9.4	***	temperature	$4.9\ 10^{-2}$	8.9	**
morphological richness	$9.4\ 10^{-3}$	11.1	**	salinity	$9.0\ 10^{-3}$	20.3	*
morphological evenness	$5.7\ 10^{-3}$	6.6	***	density	$-2.4\ 10^{-3}$	7.6	
morphological divergence	$6.0\ 10^{-3}$	4.7		oxygen	$3.6\ 10^{-2}$	18.9	***
taxonomic richness	$4.8\ 10^{-1}$	11.3	***	NO_2^-	$-1.3\ 10^{-3}$	14.1	
taxonomic evenness	$9.4\ 10^{-3}$	4.4		NO_3^-	$6.1\ 10^{-3}$	15.5	
taxonomic diversity	$1.4\ 10^{-3}$	4.4		PO_4^{3-}	$-1.6\ 10^{-3}$	18.2	*
size-mean	$2.2\ 10^{-2}$	12.6		$SiOH_4$	$-3.1\ 10^{-2}$	13.4	
-var	$9.3\ 10^{-2}$	9.4	*	POC	-3.6	16.3	***
-q25	$-5.8\ 10^{-2}$	6.3	***	PON	$-1.9\ 10^{-1}$	10.7	*
-q75	$8.3\ 10^{-2}$	11.3		Chl. a	$1.3\ 10^{-2}$	12.6	***
transparency-mean	$3.3\ 10^{-2}$	5.1	*				
-var	$3.6\ 10^{-2}$	2.3	**				
-q25	$9.9\ 10^{-3}$	2.9					
-q75	$5.3\ 10^{-2}$	2.7	***				
circularity-mean	$-4.7\ 10^{-2}$	4.1	**				
-var	$3.3\ 10^{-2}$	6.9					
-q25	$-4.2\ 10^{-2}$	2.3	*				
q75	$-3.5\ 10^{-2}$	4.2	***				
complexity-mean	$-1.2\ 10^{-2}$	2.5					
-var	$9.6\ 10^{-3}$	10.1					
-q25	$-2.8\ 10^{-3}$	10.5					
-q75	$-1.5\ 10^{-2}$	5.6					

both absolutely (MRic) and relatively (MDiv), there was an increase in transparency and elongated shapes over the spring–summer transition. Classically, the spring peak of zooplankton following the phytoplankton bloom denotes a period of high production. It is generally dominated by Copepoda, and taxonomic—and as we showed also morphological—diversity is low. With the decline of Copepoda and the increase of other taxa, notably gelatinous Appendicularia and Chaetognatha [60–62], diversity increased to stay on a high level later in the year. This increase in gelatinous plankton matches the morphological changes that we detected in the plankton community. Besides taxonomic changes, the ontogenetic development of organisms also probably increased morphological diversity towards summer: while copepodite stages of Copepoda are morphologically similar across species, their appearances as adults differ. This could explain the increase in average size and in the variability in morphological traits that we noticed (electronic supplementary material, S3). Thus, it seems that both increasing taxonomic diversity and the life cycle of dominating taxa caused the increase in morphological diversity towards the low-production, summer period.

(b) Morphological diversity and specialization over the long term

Under an impoverishment in nutrients (especially nitrate) and organic matter, the zooplankton concentration declined over the 12-year period while the community became morphologically more diverse. This resembles the trend observed from spring to summer, albeit with a lower amplitude and probably caused by different ecological mechanisms.

Here also, the increase in morphological diversity could have resulted from increasing taxonomic diversity. This has been observed for functional diversity indices, in Copepoda and aquatic macroinvertebrates [63,64]. Also, the morphological changes (increases in transparency and elongation) correspond to the taxonomic shifts in the zooplankton community at point B in recent years [61]: after a drop in zooplankton concentration in 2015, following a sudden temperature increase in summer that year, gelatinous zooplankton (notably Appendicularia and Chaetognatha, both with rather elongated body shapes) recovered, but crustacean densities remained rather low.
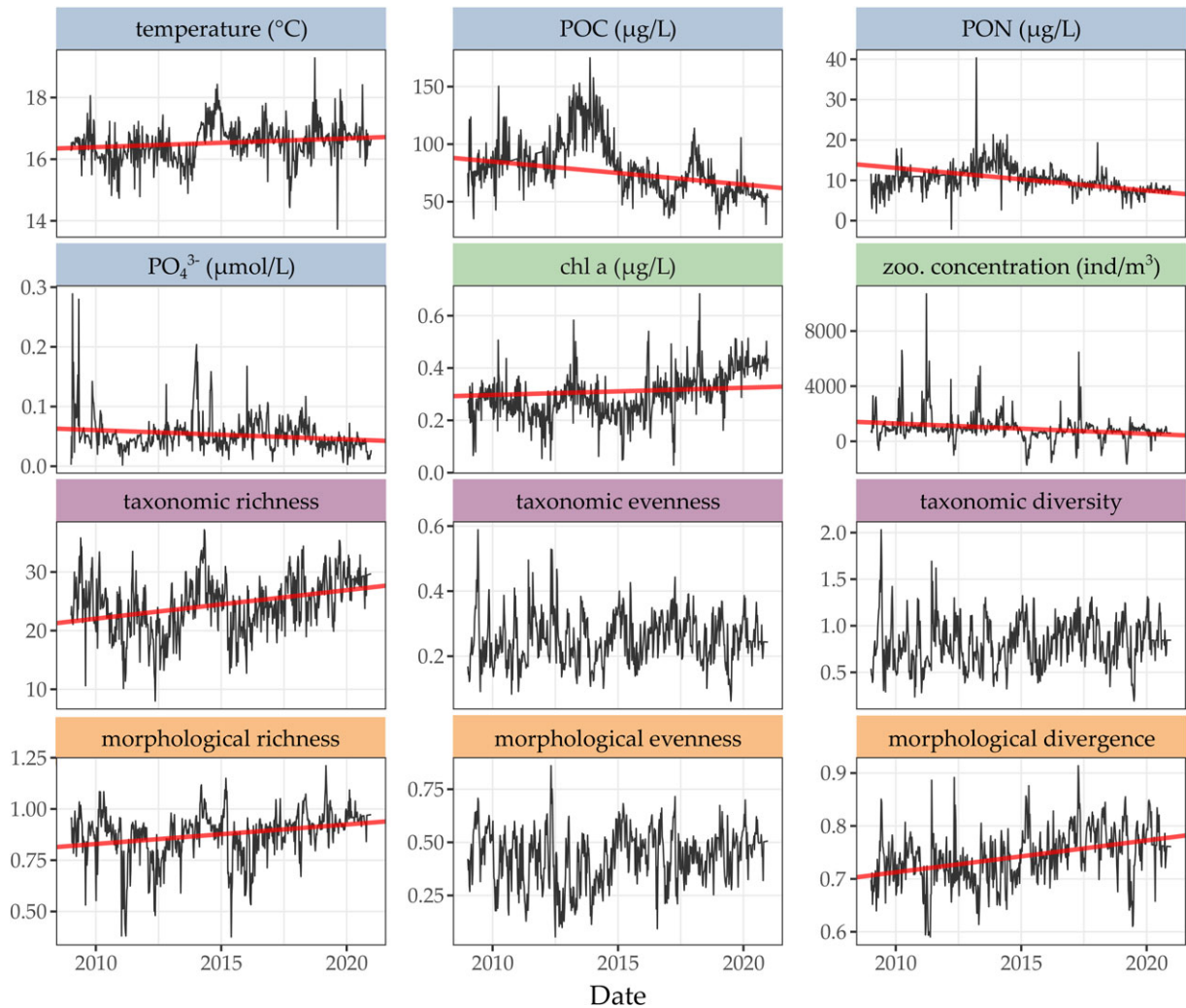
Figure 4. Weekly time series of environmental variables (temperature, POC, PON, PO_4^{3-}, chlorophyll *a*) and zooplankton concentration, taxonomic and morphological diversity indices (richness, evenness, diversity/divergence) over the years 2009–2020. Black lines are the de-seasonalized series, red lines are the significant trends (with $p < 0.05$) obtained from GLS regression.

However, while both taxonomic and morphological richness increased significantly, only morphological but not taxonomic diversity increased. This discrepancy may be partially attributable to the rather low taxonomic resolution in our study. Still, as discussed above, a higher resolution did not change the seasonal signal much. Also, when considering only Copepoda, a group morphologically more homogeneous but taxonomically diverse, we obtained morphological traits and trends in morphological diversity very similar to those of the whole community. Taxonomy therefore was unlikely to be the only driver. Finally, the fact that each morph comprised several taxa, and conversely each taxon comprising several morphs also indicates that morphology is not a mere mirroring of taxonomy. Overall, this underlines the relevance of considering diversity descriptors beyond taxonomy to detect changes in ecosystems from different perspectives [65].

In our case, a mechanism similar to that of taxonomic or functional specialization could also explain the observed pattern: diversity increases when a community shifts from generalists to more specialized taxa. Generalist or opportunistic taxa tolerate a large range of environmental conditions and/or express high growth rates, allowing them to establish their dominance in resource-rich conditions. One example is Copepoda (mostly Calanoida) during the spring bloom,

but it has also been described for grassland moths or benthic macroinvertebrates under (agricultural) eutrophication [37,66]. Such communities, dominated by generalists, often display low taxonomic and functional diversity [66,67]. Under oligotrophic conditions, specialized taxa more efficiently exploit the scarce resources, each within a narrow range of conditions, and outcompete generalists [68]. In that situation, either a larger number of taxa coexist and taxonomic diversity increases, or a similar number of functionally more diverse taxa coexist and functional diversity increases, or both. Such mechanism has often been reported to cause taxonomic or functional homogenization with increasing eutrophication, along a spatial gradient of sites, for a range of aquatic [35,36,69] and terrestrial [70] habitats. Benthic communities for example were more taxonomically heterogeneous under low nutrient and chlorophyll *a* levels, both within and among lakes [71]. Our results suggest that this also happens in time and for morphological heterogeneity.

Over the study period, increases in temperature and salinity were accompanied by an impoverishment of nutrients, thereby intensifying the already oligotrophic conditions of the Mediterranean Sea. These observations match climate models predictions [72–74]. Increased stratification of the water column reduced the depth of vertical mixing in

winter in recent years, thus preventing nutrient supply to the surface layer, as observed at two stations in the same region [75]. Contrary to those expectations, chlorophyll *a* concentration, a proxy for autotrophic phytoplankton biomass, significantly increased. However, at a nearby site phytoplankton pigment measurements by high performance liquid chromatography revealed a concomitant shift of the phytoplankton community towards smaller taxa (C Migon 2023, personal communication), of lesser nutritious quality for zooplankton [76]. Thus, even though chlorophyll *a* was increasing, the amount of food actually available to the zooplankton community, notably to Copepoda, may have decreased.

In both scenarios (taxonomic changes or morphological specialization), the increase in morphological diversity can be explained by a decline of the dominant morphologies, here associated with Copepoda, both seasonally and over the long term. Twelve years are not sufficient to disentangle inter-annual variability from climate-related effects. Still, the observed environmental trends were mostly consistent in a longer 20-year period (electronic supplementary material, S9), a time scale becoming relevant to study climate changes. Thus, the relationships between environmental forcing and zooplankton morphological diversity may extend further in time.

(c) Morphological shifts and possible functional implications

The observed increase in morphological diversity was caused by increasing variance in size and transparency as well as shifts towards higher proportions of very small, transparent and elongated organisms, on both temporal scales. A full analysis of potential changes in ecosystem functioning requires detailed (e.g. species level) taxonomic identifications, to link each species to its functional traits and describe their change through time. This is not possible with our data, but the literature suggests some relationships between morphology and ecological functions that transcend species boundaries, as discussed in the following.

Body size was the most variable morphological trait in the zooplankton community (i.e. appearing as the first principal component). Although no significant change in average body size occurred, the proportion of very small organisms and the overall variation in size increased, both for the entire community and within Copepoda. This partially supports the hypothesis that warming would 'benefit the small' and is in line with previous works reporting or projecting increasing abundances of small taxa, from phyto- and zoo-plankton to fish [32,34,77,78]. Although interspecific interactions are complex, large proportions of small body sizes, i.e. steep slopes of community size spectra, are usually associated with low transfer efficiency through the food web [79,80]. Conversely, a wider size range of (meso-)zooplankton (through increased size variability) might increase diet niche partitioning and increase trophic transfer [81,82].

Transparency is an efficient camouflage in open water [83] and a common strategy in plankton. With increased water clarity through oligotrophication, transparency probably becomes more relevant to hide from visual predators [84]. This is consistent with the increase in transparent organisms during a decrease in organic particles observed in our study, on both temporal scales. Here, one explanation of this increase, and of the trend towards more elongated

body shapes, is the shift towards Appendicularia and Chaetognatha. Given the well-defined feeding strategies of both taxa (Chaetognatha are carnivores, Appendicularia are filter-feeders), those changes could hint at functional changes in the zooplankton community. Furthermore, increasing transparency of mesozooplankton might be negatively correlated to carbon export [85], possibly because of similar taxonomic and functional changes in the community with consequences for the ocean carbon flux. This flux is affected by both zooplankton taxonomic composition and the morphology of marine snow particles [86,87], making it interesting to investigate the relationship between zooplankton morphology and particle morphology and, in consequence, carbon export.

More generally, it would be relevant to investigate how these phenotypic variations as such relate to functional diversity and ecosystem functioning, e.g. whether increasing morphological diversity has the same beneficial effects as taxonomic or functional diversity on ecosystem functions such as nutrient transfer [88], resource use efficiency [8], primary or secondary production [1,5]. A morphologically diverse community might, for example, harbour more specialized feeding strategies because of the large morphological range of prey, and changes in transparency and elongation might alter or indicate a modification of the trophic structure.

The four synthetic morphological traits we derived for a zooplankton community in the Mediterranean Sea were close to those previously identified for Copepoda in the Arctic [25] and phytoplankton in the northeastern Atlantic [22]. They were not purely driven by ZooScan imaging or limited by the measurements performed on those images since (i) the two studies above used other instruments (the Underwater Vision Profile and the Imaging Flow Cyto Bot), and (ii) the four traits were similar for a morphological space built with features computed by a deep learning model. Therefore, they seem to be important phenotypic characteristics of planktonic communities, which strengthens the hypothesis that they have a functional role.

A quantitative imaging dataset of zooplankton allowed us to synthesize traits that provide insight into a widely unused facet of biological diversity. Our approach is generic and applicable to other taxonomic groups or ecosystems, provided that standardized images of individual organisms are available. To encourage its reuse, we share general-purpose code libraries. We demonstrated that common patterns observed and/or assumed for taxonomic and functional diversity, i.e. increased diversity through specialization under less productive conditions, were also evident in morphology and on different temporal scales: seasonally and over 12 years. To our knowledge, this is only the second time this supposedly well-known link between production and diversity is demonstrated along a time series [38]. Over the long term at least, the changes in morphology did not seem attributable to taxonomy only, suggesting a direct functional role of morphological traits. If these phenotypic changes are indeed caused by the impoverishment of Mediterranean waters, this trend probably continues in the future according to climate model predictions [89].

environmental data are accessible under https://www.somlit.fr/demande-de-donnees. The code is available on GitHub https://github.com/jiho/ptb_morphodiv.

Supplementary material is available online [91].

References

1. Setubal RB, Sodré E de O, Martins T, Bozelli RL. 2020 Effects of functional diversity and salinization on zooplankton productivity: an experimental approach. *Hydrobiologia* **847**, 2845–2862. (doi:10.1007/s10750-020-04276-0)

2. Tilman D, Reich PB, Knops J, Wedin D, Mielke T, Lehman C. 2001 Diversity and productivity in a long-term grassland experiment. *Science* **294**, 843–845. (doi:10.1126/science.1060391)

3. Dederck S, Vanderstukken M, Pals A, Muylaert K, Meester LD. 2007 Plankton biodiversity along a gradient of productivity and its mediation by macrophytes. *Ecology* **88**, 2199–2210. (doi:10.1890/07-0048.1)

4. Witman JD, Cusson M, Archambault P, Pershing AJ, Mieszkowska N. 2008 The relation between productivity and species diversity in temperate–arctic marine ecosystems. *Ecology* **89**(sp11), S66–S80. (doi:10.1890/07-1201.1)

5. Korhonen JJ, Wang J, Soininen J. 2011 Productivity-diversity relationships in lake plankton communities. *PLoS ONE* **6**, e22041. (doi:10.1371/journal.pone.0022041)

6. Mittelbach GG, Steiner CF, Scheiner SM, Gross KL, Reynolds HL, Waide RB, Willig MR, Dodson SI, Gough L. 2001 What is the observed relationship between species richness and productivity? *Ecology* **82**, 2381–2396. (doi:10.1890/0012-9658(2001)082[2381:WITORB]2.0.CO;2)

7. Schmera D, Heino J, Podani J. 2022 Characterising functional strategies and trait space of freshwater macroinvertebrates. *Sci. Rep.* **12**, 12283. (doi:10.1038/s41598-022-16472-0)

8. Vallina SM, Cermeno P, Dutkiewicz S, Loreau M, Montoya JM. 2017 Phytoplankton functional diversity increases ecosystem productivity and stability. *Ecol. Model.* **361**, 184–196. (doi:10.1016/j.ecolmodel.2017.06.020)

9. Weithoff G, Rocha MR, Gaedke U. 2015 Comparing seasonal dynamics of functional and taxonomic diversity reveals the driving forces underlying phytoplankton community structure. *Freshw. Biol.* **60**, 758–767. (doi:10.1111/fwb.12527)

10. Nielsen T, Sand-Jensen K, Dornelas M, Bruun HH. 2019 More is less: net gain in species richness, but biotic homogenization over 140 years. *Ecol. Lett.* **22**, 1650–1657. (doi:10.1111/ele.13361)

11. Leruste A, Villéger S, Malet N, De Wit R, Bec B. 2018 Complementarity of the multidimensional functional and the taxonomic approaches to study phytoplankton communities in three Mediterranean coastal lagoons of different trophic status. *Hydrobiologia* **815**, 207–227. (doi:10.1007/s10750-018-3565-4)

12. Magurran AE, Dornelas M, Moyes F, Gotelli NJ, McGill B. 2015 Rapid biotic homogenization of marine fish assemblages. *Nat. Commun.* **6**, 8405. (doi:10.1038/ncomms9405)

13. Brown JH, Gillooly JF, Allen AP, Savage VM, West GB. 2004 Toward a metabolic theory of ecology. *Ecology* **85**, 1771–1789. (doi:10.1890/03-9000)

14. Kleiber M. 1932 Body size and metabolism. *Hilgardia* **6**, 315–353. (doi:10.3733/hilg.v06n11p315)

15. Hansen PJ, Bjørnsen PK, Hansen BW. 1997 Zooplankton grazing and growth: scaling within the 2-2,-μm body size range. *Limnol. Oceanogr.* **42**, 687–704. (doi:10.4319/lo.1997.42.4.0687)

16. Latli A *et al.* 2017 Long-term trends in trait structure of riverine communities facing predation risk increase and trophic resource decline. *Ecol. Appl.* **27**, 2458–2474. (doi:10.1002/eap.1621)

17. Rasconi S, Gall A, Winter K, Kainz MJ. 2015 Increasing water temperature triggers dominance of small freshwater plankton. *PLoS ONE* **10**, e0140449. (doi:10.1371/journal.pone.0140449)

18. Strecker AL, Cobb TP, Vinebrooke RD. 2004 Effects of experimental greenhouse warming on phytoplankton and zooplankton communities in fishless alpine ponds. *Limnol. Oceanogr.* **49**, 1182–1190. (doi:10.4319/lo.2004.49.4.1182)

19. Dossena M, Yvon-Durocher G, Grey J, Montoya JM, Perkins DM, Trimmer M, Woodward G. 2012 Warming alters community size structure and ecosystem functioning. *Proc. R. Soc. B* **279**, 3011–3019. (doi:10.1098/rspb.2012.0394)

20. DeLong JP *et al.* 2015 The body size dependence of trophic cascades. *Am. Nat.* **185**, 354–366. (doi:10.1086/679735)

21. Marinello MM, Bernard E. 2014 Wing morphology of Neotropical bats: a quantitative and qualitative analysis with implications for habitat use. *Can. J. Zool.* **92**, 141–147. (doi:10.1139/cjz-2013-0127)

22. Sonnet V, Guidi L, Mouw CB, Puggioni G, Ayata SD. 2022 Length, width, shape regularity, and chain structure: time series analysis of phytoplankton morphology from imagery. *Limnol. Oceanogr.* **67**, 1850–1864. (doi:10.1002/lno.12171)

23. Orenstein EC *et al.* 2022 Machine learning techniques to characterize functional traits of plankton from image data. *Limnol. Oceanogr.* **67**, 1647–1669. (doi:10.1002/lno.12101)

24. Irisson JO, Ayata SD, Lindsay DJ, Karp-Boss L, Stemmann L. 2022 Machine learning for the study of plankton and marine snow from images. *Annu. Rev. Mar. Sci.* **14**, 277–301. (doi:10.1146/annurev-marine-041921-013023)

25. Vilgrain L, Maps F, Picheral M, Babin M, Aubry C, Irisson JO, Ayata SD. 2021 Trait-based approach using in situ copepod images reveals contrasting ecological patterns across an Arctic ice melt zone. *Limnol. Oceanogr.* **66**, 1155–1167. (doi:10.1002/lno.11672)

26. Langerhans RB, Layman CA, Shokrollahi AM, DeWitt TJ. 2004 Predator-driven phenotypic diversification in *Gambusia affinis*. *Evolution* **58**, 2305–2318.

27. Pörtner HO *et al.* 2021 *IPBES-IPCC co-sponsored workshop report on biodiversity and climate change*. IPBES and IPCC. See https://www.ipbes.net/events/ipbes-ipcc-co-sponsored-workshop-biodiversity-and-climate-change.

28. Kwiatkowski L *et al.* 2020 Twenty-first century ocean warming, acidification, deoxygenation, and upper-ocean nutrient and primary production decline from CMIP6 model projections. *Biogeosciences* **17**, 3439–3470. (doi:10.5194/bg-17-3439-2020)

29. Bryndum-Buchholz A, Tittensor DP, Blanchard JL, Cheung WWL, Coll M, Galbraith ED, Jennings S, Maury O, Lotze HK. 2019 Twenty-first-century climate change impacts on marine animal biomass and ecosystem structure across ocean basins. *Glob. Change Biol.* **25**, 459–472. (doi:10.1111/gcb.14512)

30. Lotze HK *et al.* 2018 Ensemble projections of global ocean animal biomass with climate change. *bioRxiv*. 467175. See https://www.biorxiv.org/content/10.1101/467175v1 (accessed 13 January 2023).

31. Cheung WWL, Lam VWY, Sarmiento JL, Kearney K, Watson R, Pauly D. 2009 Projecting global marine biodiversity impacts under climate change scenarios. *Fish Fish.* **10**, 235–251. (doi:10.1111/j.1467-2979.2008.00315.x)

32. Daufresne M, Lengfellner K, Sommer U. 2009 Global warming benefits the small in aquatic ecosystems. *Proc. Natl Acad. Sci. USA* **106**, 12 788–12 793. (doi:10.1073/pnas.0902080106)

33. Lefort S, Aumont O, Bopp L, Arsouze T, Gehlen M, Maury O. 2015 Spatial and body-size dependent response of marine pelagic communities to projected global climate change. *Glob. Change Biol.* **21**, 154–164. (doi:10.1111/gcb.12679)

34. Moullec F, Barrier N, Drira S, Guilhaumon F, Marsaleix P, Somot S, Ulses C, Velez L, Shin YJ. 2019 An end-to-end model reveals losers and winners in a warming Mediterranean Sea. *Front. Mar. Sci.* **6**, 345. (doi:10.3389/fmars.2019.00345)

35. Chihoub S, Christaki U, Chelgham S, Amara R, Ramdane Z, Zebboudj A, Rachik S, Breton E. 2020 Coastal eutrophication as a potential driver of functional homogenization of copepod species assemblages in the Mediterranean Sea. *Ecol. Indic.* **115**, 106388. (doi:10.1016/j.ecolind.2020.106388)

36. Li Y, Wang R, Su H, Wang J, Xie P, Chen F. 2022 Eutrophication and predation mediate zooplankton diversity and network structure. *Limnol. Oceanogr.* **67**, S133–S145.

37. Zhang Y, Cheng L, Li K, Zhang L, Cai Y, Wang X, Heino J. 2019 Nutrient enrichment homogenizes taxonomic and functional diversity of benthic macroinvertebrate assemblages in shallow lakes. *Limnol. Oceanogr.* **64**, 1047–1058. (doi:10.1002/lno.11096)

38. Abonyi A, Ács É, Hidas A, Grigorszky I, Várbíró G, Borics G, Kiss K. 2018 Functional diversity of phytoplankton highlights long-term gradual regime shift in the middle section of the Danube River due to global warming, human impacts and oligotrophication. *Freshw. Biol.* **63**, 456–472. (doi:10.1111/fwb.13084)

39. Garrabou J *et al.* 2022 Marine heatwaves drive recurrent mass mortalities in the Mediterranean Sea. *Glob. Change Biol.* **28**, 5708–5725. (doi:10.1111/gcb.16301)

40. Ramírez F, Coll M, Navarro J, Bustamante J, Green AJ. 2018 Spatial congruence between multiple stressors in the Mediterranean Sea may reduce its resilience to climate impacts. *Sci. Rep.* **8**, 14871. (doi:10.1038/s41598-018-33237-w)

41. Feuilloley G, Fromentin JM, Stemmann L, Demarcq H, Estournel C, Saraux C. 2020 Concomitant changes in the environment and small pelagic fish community of the Gulf of Lions. *Prog. Oceanogr.* **186**, 102375. (doi:10.1016/j.pocean.2020.102375)

42. Motoda S. 1959 Devices of simple plankton apparatus. *Mem. Fac. Fish Hokkaido Univ.* **7**, 73–94.

43. Gorsky G *et al.* 2010 Digital zooplankton image analysis using the ZooScan integrated system. *J. Plankton Res.* **32**, 285–303. (doi:10.1093/plankt/fbp124)

44. Picheral M, Colin S, Irisson JO. 2017 *EcoTaxa, a tool for the taxonomic classification of images*. See https://ecotaxa.obs-vlfr.fr/.

45. Hartigan JA, Wong MA. 1979 Algorithm AS 136: a *K*-means clustering algorithm. *J. R. Stat. Soc. Ser. C Appl. Stat.* **28**, 100–108.

46. Villéger S, Mason NWH, Mouillot D. 2008 New multidimensional functional diversity indices for a multifaceted framework in functional ecology. *Ecology* **89**, 2290–2301. (doi:10.1890/07-1206.1)

47. Pielou EC. 1969 An introduction to mathematical ecology. *Introd. Math. Ecol.* See https://www.cabdirect.org/cabdirect/abstract/19729701428 (accessed 28 October 2022).

48. Shannon CE. 1948 A mathematical theory of communication. *Bell Syst. Tech. J.* **27**, 379–423. (doi:10.1002/j.1538-7305.1948.tb01338.x)

49. Cleveland R, Cleveland W, Terpenning I. 1990 STL: a seasonal-trend decomposition procedure based on loess. *J. Off. Stat.* **6**, 3–73.

50. Fox J, Weisberg S. 2018 *An R companion to applied regression*. Thousand Oaks, CA: Sage Publications.

51. R Development Core Team. 2022 *R: A language and environment for statistical computing*. Vienna: R Foundation for Statistical Computing. See http://www.R-project.org/ (accessed 15 April 2020).

52. Dray S, Dufour AB. 2007 The ade4 package: implementing the duality diagram for ecologists. *J. Stat. Softw.* **22**, 1–20. (doi:10.18637/jss.v022.i04)

53. Oksanen J, Blanchet FG, Friendly M, Kindt R, Legendre P, McGlinn D *et al.* 2020 vegan: community ecology package. R package version 2.5-6. 2019.

54. Grosjean P, Ibanez F, Etienne M. 2014 Pastecs: package for analysis of space-time ecological series. *R package Version* **1**, 1–3.

55. Hafen R. 2016 *Package 'stlplus' enhanced seasonal decomposition of time series by Loess, version 0.5.1*. See https://cran.r-project.org/web/packages/stlplus/index.html.

56. Pinheiro J, Bates D, DebRoy S, Sarkar D, Heisterkamp S, Van Willigen B, Maintainer R. 2017 *Package nlme: linear nonlinear mixed effect models*. See https://cran.r-project.org/web/packages/nlme/nlme.pdf.

57. Hadley Wickham RF, Henry L, Müller K. 2017 dplyr: a grammar of data manipulation. R package version 0.7. See https://cran.r-project.org/web/packages/dplyr/index.html.

58. Wickham H, Chang W. 2016 *ggplot2. R package version 2.2.1*. See https://cran.r-project.org/web/packages/ggplot2/index.html.

59. Kassambara A, Mundt F. 2021 *Factoextra: extract and visualize the results of multivariate data analyses. R Package Version 1.0.7*. See https://cran.r-project.org/web/packages/factoextra/readme/README.html.

60. Calbet A, Garrido S, Saiz E, Alcaraz M, Duarte CM. 2001 Annual zooplankton succession in coastal NW Mediterranean waters: the importance of the smaller size fractions. *J. Plankton Res.* **23**, 319–331. (doi:10.1093/plankt/23.3.319)

61. Feuilloley G, Fromentin JM, Saraux C, Irisson JO, Jalabert L, Stemmann L. 2022 Temporal fluctuations in zooplankton size, abundance, and taxonomic composition since 1995 in the North Western Mediterranean Sea. *ICES J. Mar Sci.* **79**, 882–900. (doi:10.1093/icesjms/fsab190)

62. Fullgrabe L, Grosjean P, Gobert S, Lejeune P, Leduc M, Engels G, Dauby P, Boissery P, Richir J. 2020 Zooplankton dynamics in a changing environment: a 13-year survey in the northwestern Mediterranean Sea. *Mar. Environ. Res.* **159**, 104962. (doi:10.1016/j.marenvres.2020.104962)

63. Becker ÉC, Mazzocchi MG, de Macedo-Soares LCP, Costa Brandão M, Santarosa Freire A. 2021 Latitudinal gradient of copepod functional diversity in the South Atlantic Ocean. *Prog. Oceanogr.* **199**, 102710. (doi:10.1016/j.pocean.2021.102710)

64. Schmera D, Heino J, Podani J, Erős T, Dolédec S. 2017 Functional diversity: a review of methodology and current knowledge in freshwater macroinvertebrate research. *Hydrobiologia* **787**, 27–44. (doi:10.1007/s10750-016-2974-5)

65. Villéger S, Grenouillet G, Brosse S. 2014 Functional homogenization exceeds taxonomic homogenization among European fish assemblages. *Glob. Ecol. Biogeogr.* **23**, 1450–1460. (doi:10.1111/geb.12226)

66. Mangels J, Fiedler K, Schneider FD, Blüthgen N. 2017 Diversity and trait composition of moths respond to land-use intensification in grasslands: generalists replace specialists. *Biodivers. Conserv.* **26**, 3385–3405. (doi:10.1007/s10531-017-1411-z)

67. Villéger S, Miranda JR, Hernández DF, Mouillot D. 2010 Contrasting changes in taxonomic vs. functional diversity of tropical fish communities after habitat degradation. *Ecol. Appl.* **20**, 1512–1522. (doi:10.1890/09-1310.1)

68. Clavel J, Julliard R, Devictor V. 2011 Worldwide decline of specialist species: toward a global functional homogenization? *Front. Ecol. Environ.* **9**, 222–228. (doi:10.1890/080216)

69. Jeppesen E, Peder Jensen J, SØndergaard M, Lauridsen T, Landkildehus F. 2000 Trophic structure, species richness and biodiversity in Danish lakes: changes along a phosphorus gradient. *Freshw. Biol.* **45**, 201–218. (doi:10.1046/j.1365-2427.2000.00675.x)

70. Chisté MN, Mody K, Kunz G, Gunczy J, Blüthgen N. 2018 Intensive land use drives small-scale homogenization of plant- and leafhopper communities and promotes generalists. *Oecologia* **186**, 529–540. (doi:10.1007/s00442-017-4031-0)

71. Donohue I, Jackson AL, Pusch MT, Irvine K. 2009 Nutrient enrichment homogenizes lake benthic assemblages at local and regional scales. *Ecology* **90**, 3470–3477. (doi:10.1890/09-0415.1)

72. Adloff F *et al.* 2015 Mediterranean Sea response to climate change in an ensemble of twenty first century scenarios. *Clim. Dyn.* **45**, 2775–2802. (doi:10.1007/s00382-015-2507-3)

73. Pagès R, Baklouti M, Barrier N, Ayache M, Sevault F, Somot S, Moutin T. 2020 Projected effects of climate-induced changes in hydrodynamics on the biogeochemistry of the Mediterranean sea under the RCP 8.5 Regional Climate Scenario. *Front. Mar. Sci.* **7**, 563615. (doi:10.3389/fmars.2020.563615)

74. Soto-Navarro J *et al.* 2020 Evolution of Mediterranean sea water properties under climate change scenarios in the Med-CORDEX ensemble. *Clim. Dyn.* **54**, 2135–2165. (doi:10.1007/s00382-019-05105-4)

75. Margirier F *et al.* 2020 Abrupt warming and salinification of intermediate waters interplays with decline of deep convection in the Northwestern Mediterranean Sea. *Sci. Rep.* **10**, 20923. (doi:10.1038/s41598-020-77859-5)

76. Jagadeesan L, Jyothibabu R, Arunpandi N, Parthasarathi S. 2017 Copepod grazing and their impact on phytoplankton standing stock and production in a tropical coastal water during the different seasons. *Environ. Monit. Assess.* **189**, 105. (doi:10.1007/s10661-017-5804-y)

77. Avaria-Llautureo J, Venditti C, Rivadeneira MM, Inostroza-Michael O, Rivera RJ, Hernández CE, Canales-Aguirre CB. 2021 Historical warming consistently decreased size, dispersal and speciation rate of fish. *Nat. Clim. Change* **11**, 787–793. (doi:10.1038/s41558-021-01123-5)

78. Uszko W, Huss M, Gårdmark A. 2022 Smaller species but larger stages: warming effects on inter- and intraspecific community size structure. *Ecology* **103**, e3699. (doi:10.1002/ecy.3699)

79. Atkinson A *et al.* 2021 Increasing nutrient stress reduces the efficiency of energy transfer through planktonic size spectra. *Limnol. Oceanogr.* **66**, 422–437. (doi:10.1002/lno.11613)

80. Toruan RL, Coggins LX, Ghadouani A. 2021 Response of zooplankton size structure to multiple stressors in urban lakes. *Water* **13**, 2305. (doi:10.3390/w13162305)

81. García-Comas C, Sastri AR, Ye L, Chang CY, Lin FS, Su MS, Gong G-C, Hsieh C. 2016 Prey size diversity hinders biomass trophic transfer and predator size diversity promotes it in planktonic communities. *Proc. R. Soc. B* **283**, 20152129. (doi:10.1098/rspb.2015.2129)

82. Ye L, Chang CY, García-Comas C, Gong GC, Hsieh C. 2013 Increasing zooplankton size diversity enhances the strength of top-down control on phytoplankton through diet niche partitioning. *J. Anim. Ecol.* **82**, 1052–1061. (doi:10.1111/1365-2656.12067)

83. Johnsen S. 2001 Hidden in plain sight: the ecology and physiology of organismal transparency. *Biol. Bull.* **3**, 301–318. (doi:10.2307/1543609)

84. Williamson CE, Fischer JM, Bollens SM, Overholt EP, Breckenridge JK. 2011 Toward a more comprehensive theory of zooplankton diel vertical migration: integrating ultraviolet radiation and water transparency into the biotic paradigm. *Limnol. Oceanogr.* **56**, 1603–1623. (doi:10.4319/lo.2011.56.5.1603)

85. Perhirin M, Gossner H, Godfrey J, Johnson R, Blanco-Bercial L, Ayata SD. In press. Morphological and taxonomic diversity of mesozooplankton is an important driver of carbon export fluxes in the ocean. *Mol. Ecol. Resour.*

86. Taucher J, Stange P, Algueró-Muñiz M, Bach LT, Nauendorf A, Kolzenburg R, Büdenbender J, Riebesell U. 2018 *In situ* camera observations reveal major role of zooplankton in modulating marine snow formation during an upwelling-induced plankton bloom. *Prog. Oceanogr.* **164**, 75–88. (doi:10.1016/j.pocean.2018.01.004)

87. Trudnowska E, Lacour L, Ardyna M, Rogge A, Irisson JO, Waite AM, Babin M, Stemmann L. 2021 Marine snow morphology illuminates the evolution of phytoplankton blooms and determines their subsequent vertical export. *Nat. Commun.* **12**, 2816. (doi:10.1038/s41467-021-22994-4)

88. Ye L, Chang CW, Matsuzaki SI, Takamura N, Widdicombe CE, Hsieh CH. 2019 Functional diversity promotes phytoplankton resource use efficiency. *J. Ecol.* **107**, 2353–2363. (doi:10.1111/1365-2745.13192)

89. Cos J, Doblas-Reyes F, Jury M, Marcos R, Bretonnière PA, Samsó M. 2022 The Mediterranean climate change hotspot in the CMIP5 and CMIP6 projections. *Earth Syst. Dyn.* **13**, 321–340. (doi:10.5194/esd-13-321-2022)

90. Sorbonne Université/CNRS - Institut de la Mer de Villefranche (IMEV), Sorbonne Université/CNRS - Laboratoire d'Océanographie de Villefranche (LOV). 2020 Plankton community in WP2 net (200µm), Point B, Villefranche-sur-Mer, France. (https://doi.org/10.14284/473)

91. Beck M, Cailleton C, Guidi L, Desnos C, Jalabert L, Elineau A, Stemmann L, Ayata S-D, Irisson J-O. 2023 Morphological diversity increases with decreasing resources along a zooplankton time series. Figshare. (doi:10.6084/m9.figshare.c.6922519)